Project Acronym/ Acronimo del progetto:

INTEGRIDS

Project title:

Electric and thermal grids integration with energy flexible building

Titolo del progetto:

Studio dell'integrazione di reti elettriche e termiche con la flessibilità energetica degli edifici

Deliverable name	Osservabilità delle reti energetiche e modelli previsionali
Deliverable N°.	D6.1
Task	6.2
Author of the deliverable: Approved by:	Marco Pierro, Grazia Barchi, Matteo Giacomo Prina David Moser
Due date	31/03/2019

efre·fesr Südtirol · Alto Adige
Europäischer Fonds für regionale Entwicklung
Fondo europeo di sviluppo regionale
EUROPEAN UNION
AUTONOME PROVINZ BOZEN SÜDTIROL
PROVINCIA AUTONOMA DI BOLZANO ALTO ADIGE

Table of Contents

Executive summary

Questo report descrive come modelli di previsione di generazione di impianti fotovoltaici possano essere utilizzati per valutare l'osservabilità della rete in termini di sbilanciamenti energetici tra domanda e generazione. In particolare, attualmente la grande variabilità di fonti rinnovabili quali il fotovoltaico e l'eolico dipendono dalle condizioni meteorologiche oltre che dal posizionamento. In questo studio si è studiato l'impatto della generazione solare nella rete di distribuzione dal punto di vista di accuratezza ed incertezza della previsione del giorno prima. In questo contesto, una maggiore osservabilità della rete in termini di generazione, implica una riduzione degli sbilanciamenti e minori riserve che dovrebbero essere mantenute per il giorno successivo alfine di compensare lo squilibrio e stabilizzare la tensione e la frequenza di rete. Lo studio è stato effettuato su un'area della regione Alto Adige sotto il controllo di un DSO locale utilizzando dati di generazione di carico e fotovoltaico con una granularità di un'ora e riferiti al 2015. Questi i principali risultati dello studio.

In assenza di generazione FV, la domanda elettrica può essere prevista con una precisione accettabile anche con un semplice metodo statistico basato su dati storici. Pertanto, questo metodo genera valori ragionevoli di squilibrio e riserve. In particolare, il metodo statistico e un approccio probabilistico più sofisticato (che ci rende più precisi nella previsione del fotovoltaico) mostrano un vantaggio alternativo. Il primo ottiene una stima di riserva successiva più affidabile (vale a dire un rischio inferiore al previsto) e una minore necessità di riserve di rampa. Il secondo raggiunge uno squilibrio più basso e le seguenti riserve. Anche con solo il 7% della penetrazione del fotovoltaico, lo squilibrio e le riserve previsti dal metodo di previsione statistica aumentano considerevolmente a causa della generazione solare. Contenere squilibri e riserve l'uso dell'approccio probabilistico ha fornito vantaggi ragionevoli. Riduce lo squilibrio del 24% e le seguenti riserve del 32%. Tuttavia, anche in questo caso, il modello probabilistico è leggermente meno affidabile e impone l'uso di riserve di rampe più elevate rispetto all'approccio statistico.
A un livello più alto di penetrazione del fotovoltaico, l'uso di modelli PV e di carico netto più accurati diventa essenziale per limitare squilibri e riserve. In effetti, con la crescita della penetrazione solare, lo squilibrio e le riserve ottenute con l'approccio statistico aumentano notevolmente. In questo caso, l'approccio probabilistico sarà sempre il metodo migliore sia in termini di squilibrio, a seguito dell'affidabilità delle riserve, dell'ammontare delle riserve e delle rampe.
Nella parte conclusiva del report viene introdotto il concetto di osservabilità della rete elettrica relativamente al problema della stima dello stato e di come questi due concetti sono fondamentali per la buona operatività e controllo della rete. Vengono introdotte anche in forma prospettica le misure sincronizzate per le smart grid e come queste associate ad inverte fotovoltaici possano migliorare sia l'osservabilità che l'accuratezza della stima dello stato.

1 Introduction

Variable renewable energy generation (VG) as wind and solar, depends on meteorological conditions and at the moment cannot be controlled. From the point of view of observability of regional consumption, the VG acts as lack of energy need modifying the profile of the electric demand (load). In presence of VG, not the load but only the residual load (net load) can be observed. This phenomenon is known as load shadowing effect. Therefore, VG introduces in the electric demand a dependence on the solar and wind availability so that it becomes more and more intermittent and hardly predictable.

Error! Reference source not found. shows the changes of the monthly average daily profile of the net load with respect to the electric demand induced by the solar power production. It can be observed how the PV generation can completely modify the daily load profile, even at this level of penetration. In particular, it removes the load peak during summer and increase the daily power ramps in the morning and in the afternoon during the others seasons.

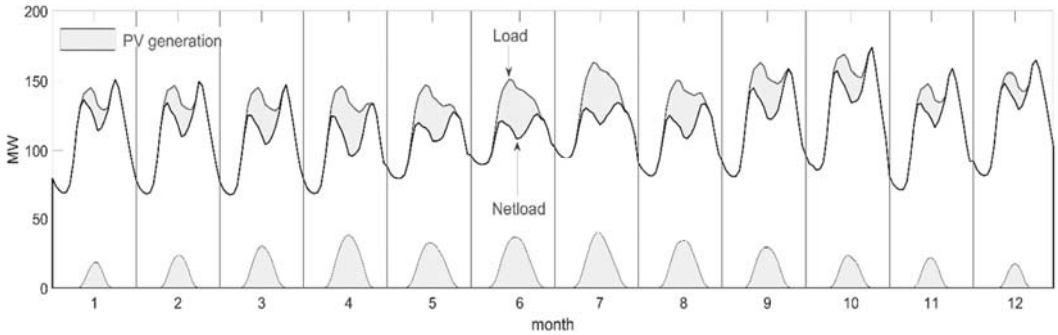

Figure 1: monthly average of the daily of the load, net load and PV generation of region in the North of Italy during the year 2015.

The variability of the load is related to the actions of consumers in the grid, the variation in demand is smooth and the occurrences of a sudden significant change is negligible so that the statistical behaviour of the load can be easily understood. Therefore, the load prediction (from minute to day-ahead horizon) and its related uncertainty, can be effectively computed also using well established statistical methods based on long time series of historical data. On the contrary, the net load forecast needs much more complex methods in continuous evolution that should take into account the prediction of the meteorological conditions. Indeed, these methods make use of Numerical Weather Prediction (NWP) and sophisticate machine learning techniques to forecast wind and solar generation. In any case, the net load forecast leads to lower accuracy and higher uncertainty with respect to the load prediction, especially at high VG conditions.

As a consequence, the imbalance between the electric demand and the power supply (net load forecast) and its related costs on the energy imbalance market increases with the growing of wind and solar penetration. Moreover, also the operating reserves are intrinsic related to the uncertainty of the net load forecast, since they are the flexible capacity that should be held to accommodate the day head imbalance. Therefore, large share of VG implies high imbalance uncertainty and accordingly high amount of reserves. In particular, using the reserves general classification of Ela et al. (2011) (figure 1), the accuracy and the uncertainty day ahead forecast

of the net load define the amount of the imbalance and following reserves (reserve related to the load following).

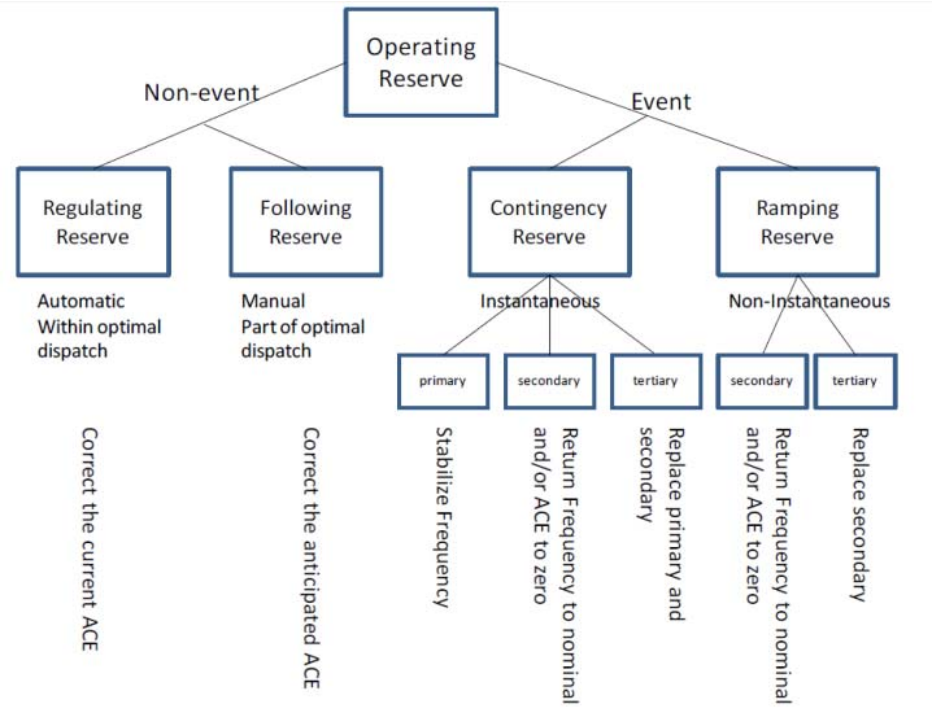

Figure 2: General classification of operating reserves from [1].

Moreover, given a certain imbalance uncertainty, the reserves "reliability" is the probability that a given amount of reserves will be able to compensate the current imbalance as well as the "risk" is the probability that the allocated reserves are not enough to balance the grid (1-reliability). For following reserves usually, a 5% of risk is assumed as an economic cost-benefit threshold. The rare but sever imbalance events that cannot be arrange by the following reserves should be compensate by the ramping reserves. The amount of ramping reserve is related to the expected risk as well to errors in following reserve assessment. These errors are due to lower uncertainty than expected i.e over confidence of the method used for reserve estimation.

For the above mentioned reasons, grid observability can be evaluated also in terms of net load forecast accuracy and uncertainty.

2 State of the art

2.1 PV forecasting to enhance grid observability

Whereas there is an extensive body of literature on load forecasting [2, 3], only recently did PV power predictions become included in these load forecast models.

In [4] the impact of PV penetration on the 15 minutes and 1-hour forecast of a micro-grid net-load is analysed. Kaur et al. (2016a) analysed the performance of PV power forecasts with several data-driven methods for hour-ahead net-load predictions in the same micro grid of the previous work. In (Kaur et al. 2016b) the benefits of using solar forecasting (in term of probability of imbalance) in the Western Interconnection dispatch energy market was quantified -- authors compared different data-driven forecast models from 5 minutes to 24 hours ahead (with different time resolutions) for 1 MW PV generation. Pierro et al. (2018) built up several models

to predict the day-ahead power transmission at regional level, but in these works no uncertainty assessment was provided. In [5] the economic valorisation on the Iberian balancing energy market of the day-ahead imbalance of a single PV plant (1.86 MWp) was computed using a reference and several forecast models and the value of the accuracy improvement with respect to the reference was provided. In [6] and [7] the imbalance costs or revenues for the owner of a single wind and PV farm of 3.6 MW and 960 kWp according to the Italian regulation of the balancing energy market are computed. Nevertheless, in [7] the prices on the DAM and BEM are assumed to be constant during the year, therefore the resulting economic evaluation is very poor. All the above mentioned papers underline the advantage of using accurate PV power forecasts to achieve energy imbalance reduction and cost saving.

In [8], the economic impact of solar power generation at different grid penetration was analysed as a function of forecast accuracy for ISO-NE. The authors analysed the costs of operational electricity generation, electricity generation from the fast start and lower efficiency power plants, ramping of all generators, start and shutdown costs, and solar power curtailment. From this analysis, they derived the value of the accuracy improvement of PV forecasting. Similar investigation on the PV and wind integration into the CASIO electric grid can be found in (Shaker, Zareipour and Wood 2016). In this paper, the authors simulate different penetration scenarios and analyse the average supply/demand daily shapes, load and net load factors, duration curves, volatility, and hourly ramps.

Furthermore, the needs to develop more effective methods to planning reserves that incorporate the solar and wind uncertainty is well explained in (Bucksteeg, Niesen and Weber 2016, Dobschinski, et al. 2017). Authors claim the transition from static reserve allocation to dynamic reserve prediction. The first is traditionally obtained by statistical approaches that produce a constant uncertainty regardless the meteorological conditions, the second can be achieved by probabilistic methods that take into account the variability of the wind and solar generation.

Probabilistic methods aim to provide either the probabilistic distribution of the forecast value or the probabilistic distribution of the forecast errors. The first approach: Probabilistic Power Forecast (PPF) is focused on informing about the distribution of potential events through a set of conditional probability density functions or ensemble of a statistically relevant number of alternative forecasts obtained through one or more models. It provides at the same time the best forecast (the expected or median value of the distribution) and the forecast uncertainty. The second approach: Probabilistic Errors Forecast (PEF) is based on a previously computed best forecast (also called “point” or “deterministic” forecast). It infers the distribution of the forecast errors from historical data to provide the prediction intervals in which the actual value is expected to lie with a certain level of confidence. Both the approaches can be classified as parametric or non-parametric methods depending on if a similarity between the distribution of the forecast and a known parametric distribution is assumed or not.

The application of these methods for a better operating reserve assessment in case of high wind penetration has been explored in the recent year. In the notable work (Ela, Milligan and Kirby 2011), a comprehensive review of large-scale renewable integration studies and academy researches, aimed to evaluate the effects of large wind generation on operating reserve and to explore new probabilistic methods for reserve assessment is reported. In [9, 10, 11, 12, 13], the authors compared traditional methods for reserve assessment with dynamic reserve allocation obtained by probabilistic approaches. They considered several case studies in Europe, USA and Canada, analysing the reserves required at different wind penetrations and forecast horizon.

Unlike the wind integration issue, how to incorporate probabilistic solar prediction into the net load forecast model is still not deeply investigated. Zhang et al.(2015) used the prediction of

solar forecast errors to compute the additional day-ahead reserve due to solar penetration and to assess the improvement in forecast accuracy that should be reached to obtain the 25% of costs reserve reduction. They analysed two regional case studies: the area under control of Independent System Operator–New England (ISO-NE) and the area controlled by the California–ISO (CAISO), and considered multiple forecast time horizons: 1-2 day ahead, 1-4 hours ahead and 15 minute ahead according to the local BEMs. In the project "A Multi-scale, Multi-Model, Machine-Learning Solar Forecasting Technology" that involved several electrical utility the need to use the uncertainty of the PV power forecast to quantify the increasing in the operating reserve due to the distributed generation was pointed out [14]. Nevertheless, these two studies, take in to account only the impact of the PV generation uncertain on the expected energy reserves regardless the uncertainty of the load forecasting. Van der Meer et al. (2018a), in their notable work, built up several probabilistic models using two different techniques to predict the solar power, electricity consumption and net load of a PV distributed fleet in the city of Sydney. They analyse the effect of seasons, aggregation and penetration on the prediction intervals of PV power, load and net load. Wu et al. (2015) estimate the economic impact on energy reserves of wind and solar uncertainty and variability for a utility in the southwestern United States (Arizona Public Service Company).

2.2 Regional PV forecast models

The starting point for Regional PV power estimation and forecast is the so-called bottom-up strategy. It consists in the estimation or forecast of all the distributed PV plants in the considered area. Nevertheless, it requires a large computational and data handling effort. Indeed, models should be implemented for each plant (even if the distance between two plants is lower than the spatial resolution of the irradiance or NWP data) and then the models should run for all the distributed systems. Moreover, when there are not enough historical data to train machine learning algorithms, a physical based models must be adopted. Nevertheless, it often happens that some system information needed for this physical models set up (such as orientation and tilt or module characteristic) are unknown. For these reasons, ongoing research is focused on upscaling methods that allow the estimation and forecast of distributed power of aggregates of PV plants through simplified approaches that reduce the computational effort and require less information on the PV fleet. For example, in [15] was proposed four different up-scaling method that can be used according to different plant information and data availability scenarios. In [16] was developed a data-driven model for regional PV power forecast that only requires the whole installed capacity and the historical PV generation in the controlled area for model's training.

Upscaling methods are mainly based on the selection of a subsets of PV plants with a power output that can be considered representative of the regional photovoltaic production. Then the forecast of the subsets power output are rescaled taking into account the subsets capacity and total capacity to obtain the regional prediction.

Several strategies has been developed in order to select the representative subsets. In (Lorenz , Hurka and Karampela , et al. 2008), two different random selection were tested. In the first the spatial distribution of the selected subsets should reflect the regional distribution while in the second just a uniform distribution of selected system was chosen. In (Lorenz, Scheidsteger and Hurka 2011) and (Lorenz, Heinemann and Kurz 2012) a subsets selection was proposed so that their distribution with respect to the location, installed capacity and system characteristics (plane orientation and technology) reflects the distribution of the whole ensemble. In [15] for the selection of representative subsets a stratified sampling method according to installed capacity and PV system location was developed.

Another upscaling method considered the PV generation in the controlled area as it was produced by a virtual PV plant. Then, the power output of this virtual plant is directly forecast by machine learning algorithms as reported in [16].

Only recently, a hybrid upscaling strategy between the two above mentioned approaches has been tested. Instead of sampling strategy, clustering methods were used for spatial grouping of PV plants and then the power output of each cluster is considered produced by a virtual PV plant and directly predicted by deterministic or machine learning models [17].

Moreover, the accuracy of regional forecast is greatly improved with respect to single site forecast due to the "ensemble smoothing effect". This effect is related to the forecasting errors correlation, the PV capacity distribution and the number of systems in the controlled area. The errors correlation between sites decreases with the distance (or with the size of the area) thus the regional forecast accuracy can be improved even by 50% with respect to the accuracy of single plant power prediction. For this reason, the performance of each site forecast only slightly affects the performance of regional prediction so that up-scaling methods can achieve similar accuracy of the bottom-up approach.

As mentioned in the previous subsection, to improve reserves assessment, it not regional PV forecast uncertainty should be provided. There for a probabilistic methods has to be adopted.

In the last few years, these methods were developed and tested not only to predict wind generation but also for solar irradiance and PV power forecast. Considering day ahead predictions, one of the first notable paper that deals with forecast uncertainty was (Lorenz et al. 2009). The authors adopted a parametric PEF methods, predicting the standard deviation of the irradiance forecast errors as a function of the sun elevation and of the forecasted clear sky index and the forecast errors are assumed normally distributed. The standard deviation was statistically computed on the fly using a moving windows of 30 days of historical data. Similar approach can be found in (Marquez and Coimbra 2011) for solar irradiance predictions (global and direct components) and in [18] for site PV power forecast. In these works, authors predicted the standard deviation of the forecast errors using a neural network model but still they assumed the normal error distribution. The same method was adopted, in [19] to compute the regional PV power prediction intervals but, in this case, a correction that took into account the deviation of the PDF of the errors from the normal distribution was built up. Ohtake et al. (2014) also adopted PEF approach based on statistical method. They constructed a look-up table of the forecast errors between the NWP (from the Japan Meteorological Agency) and ground measurements to provide the prediction intervals of the day-ahead irradiance forecast of a region in Japan. In [20], two parametric PEF methods to predict the day-ahead generation of two single PV plant were developed. These methods were based on the assumption that, for a given hour of the previous 60 days similar predicted meteorological conditions would produce similar forecast errors. The PDF of these errors was then fitted by a Gaussian and Laplacian distributions minimizing the maximum likelihood. In the same way, Fonseca et al. (2018) built up three parametric and one non-parametric methods to predict the generation of a PV fleet. In this case, Gaussian, Laplacian and hyperbolic distributions were compared with the experimental PDF derived directly from the historical data. In (Bacher, Madsen and Nielsen 2009), a non-parametric PPF approach was applied. They built up a quantile regression model to predict 1-36 hours ahead generation of a PV fleet, avoiding any assumption on parametric power distribution. Two quintiles regression models that make also use of NWP ensemble (from Meteo France's ensemble NWP system) were tested and compared in [21]. Linear quintile regression model and quantile regression forest were built to provide the 2-day ahead power forecast of PV fleets in two French counties. Quantile regression forest was also used in [22] to predict the day ahead power generation of five utility scale PV plants. The same authors in [23] compared the non-parametric method (previously developed) with a parametric method based on a physical model that derives the PV power from the NWP variables. Nevertheless, in this paper is not clear how prediction intervals of the non-parametric approach have been computed. Sperati et al. (2016) used 51 NWP forecasts coming from the Ensemble Prediction

System of ECMWF to predict the PDF of the power generated by three different solar farms in Italy with a forecast horizon between 0 and 72 hours ahead. A Neural Network model transforms each NWP forecast in PV power. Then, two different statistical methods are used to calibrate the 51 power forecasts and finally the experimental CDF is computed using the calibrated ensemble.

Since the majority of works appeared in the last four years, the probabilistic methods for solar power generations forecasting is still considered a not completely mature technology. Indeed, only recently in literature a common agreement on the metrics to assess the accuracy of the different methods is coming out. Besides, the two approaches PPF and PEF usually require the use of different key performance indexes. Moreover, unlike the point forecast, only few of the abovementioned works compute a reference probabilistic model and, in any case, there is not a well established persistence model that can be used to compare different probabilistic approaches. Zamo et al. (2014b) adopted the climatological persistence even if it is not clear how they computed this benchmark model. Sperati et al. (2016) and Fonseca et al. (2015) used a persistence model based on the power distribution generated, in a given hour, during a certain amount of previous days. For these reasons, is still very difficult to compare the different probabilistic approaches when tested in different locations and years and/or different performance metrics are used.

An overview on the techniques and metrics used in probabilistic solar forecasting can be found in the excellent reviews (Van der Meer, Widén and Munkhammar 2018b, Yang, et al. 2018).

3 Probabilistic Net load forecast methods for imbalance and reserve assessment

Eurac Research institute developed several forecasting methods to predict the net load of a part of South Tyrol Region under the control of a local DSO (Edyna Srl). These methods were used to assess the imbalance and the reserves of the controlled area at different levels of PV penetration and to quantify the energetic and economic benefit derived by the use of accurate PV forecast with respect to simple statistical approaches. These reference approaches are based on a persistence and smart persistence models denoted by (P and SP). The PV generation forecast was obtained by a novel upscaling procedure.

The developed net load probabilistic methods follow a probabilistic error forecast approach (PEF) so that it make use of point prediction.

The net load point forecast require the prediction of the load and the PV power, since the net load results from the difference between the load and the distributed PV generation:

$$P_{Netload} = P_{load} - P_{PV} \quad (1)$$

The load forecast is obtained using a Seasonal Auto-Regressive Integrated Moving Average model (SARIMA), [24]:

$$\left[\phi_p(B)\,\nabla^d\ \Phi_P(B)\,\nabla_s^D\right] P_{Load}^{SARIMA}(h+1) = c + \left[\theta_q(B)\,\Theta_Q(B)\right] e(h+1) \quad (2)$$

where $P_{Load}(h)$ is the load time series, $e(h)$ is the forecast error at the time t (supposed a white noise), s =168 is the weakly seasonality period, B $P_{Load}(h) = P_{Load}(h-1)$ is the back shift operator and each term of equation 6 represents a single model or operation.

The upscaling method used for the day-ahead power forecast (with hour granularity) consists of three different steps. First, an unsupervised clustering algorithm (k-mean) is used to group the PV plants and to find the best representative points of each cluster

(centroids)[1]. Then the numerical weather prediction data, centered on the centroids, is pre-processed with the principal component analysis (PCA). Finally, to predict the regional PV generation and then an ensemble of artificial neural networks (ANNsE) that makes use of the pre-processed NWP, is applied.

The model, named NN, can be expressed as:

$$P_{PV}^{NN}(h+24 \mid X) = f^{(2)}(W^{(2)} f^{(1)}(W^{(1)} X + b^{(1)}) + b^{(2)}) \quad (3)$$

where (i = 1, 2) is the layer index, X is the input features vectors, $f^{(i)}$ are transfer functions while the weights matrices ($W^{(i)}$) and the bias ($b^{(i)}$) are the coefficients that should be estimated during the training and validation phase, P_{PV}^{NN} is the day ahead PV power forecast (normalized by the installed capacity).

The PV forecast upscaling method is summarized in **Error! Reference source not found.**.

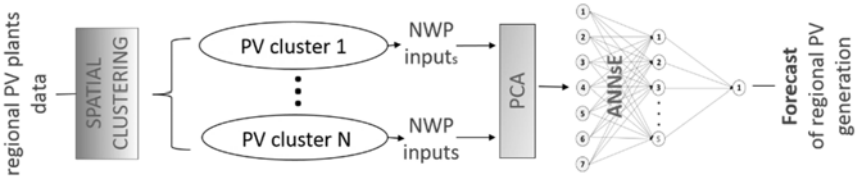

Figure 3: Upscaling method for the regional PV power forecast.

Finally, the forecast of the net load, denoted for brevity ARINN, is simply obtained from equation (1):

$$P_{Netload}^{ARINN}(h+24) = P_{Load}^{SARIMA}(h+24) - P_n \; P_{PV}^{NN}(h+24) \quad (3)$$

where P_n is the installed PV nominal capacity.

3.1 Net load probabilistic forecast

To evaluate the reserves, two different forecasts of the net load should be provided: $P_{Netlod\_up}^{for}$ and $P_{Netlod\_low}^{for}$. The power forecast upper bound ($P_{Netlod\_up}^{for}$) is the maximum expected upward regulation while the lower bound ($P_{Netlod\_low}^{for}$) is the minimum expected downward regulation. Fixing the reserve reliability at 95%, as in [25, 14, 26] , these patterns define the prediction interval (PI) in which the net load of the next day can be found with 95% of probability, i.e. the forecast uncertainty associated to the 95% of nominal confidence (PINC):

$$Prob\left(P_{Netlod\_up}^{for} \geq P_{Netlod\_low}^{actual} \geq P_{Netlod\_low}^{for}\right) = 0.95 \quad (4)$$

The energy reserve depends on the forecast accuracy and on the procedure used for the PI computation. In this sub section, the methods for PI assessment are described.

Two different non-parametric probabilistic methods for PI computation were built. These non-parametric methods are based on the ARINN net load forecast, on the prediction of the standard deviation of the forecast errors and on the forecast of experimental cumulative distribution of the errors. Finally, following the multi model approach tested in [18], an optimal blending of the two probabilistic forecast were tested.

1. The fist method denoted by ARINN/E consists in two forecast steps:

computation net load point forecast;

computation the PIs by the prediction of experimental CDF of the forecast error from historical data.

This procedure leads to a PI computation model that can be expressed by the following equation:

$$\begin{cases} \mathrm{P}^{\mathrm{ARINN/E}}_{\mathrm{Netload\_up}}(\mathrm{t}+24) = \mathrm{P}^{\mathrm{ARINN}}_{\mathrm{Netload}}(\mathrm{t}+24) - \mathrm{Q}_{(1-\mathrm{NC})/2} \\ \mathrm{P}^{\mathrm{ARINN/E}}_{\mathrm{Netload\_low}}(\mathrm{t}+24) = \mathrm{P}^{\mathrm{ARINN}}_{\mathrm{Netload}}(\mathrm{t}+24) - \mathrm{Q}_{(1+\mathrm{NC})/2} \end{cases} \quad (5)$$

where $\mathrm{P}^{\mathrm{ARINN}}_{\mathrm{Netload}}$ is the ARINN forecast, $\mathrm{Q}_{(1\pm\mathrm{NC})/2}$ are the quantiles of the eCDF of order $(1 \pm \mathrm{NC})/2$ and $\mathrm{NC} = 0.95$ is the nominal confidence of the PI.

2. The second method denoted by ARINN/S allows a dynamic PI computation and consists in three forecast steps:

computation the net load forecast;

prediction of standard deviation of the error ($\boldsymbol{\sigma_{NL}}$);

computation the PIs by the prediction of experimental CDF of the normalized forecast error.

This PI computation method, can be expressed as follows:

$$\begin{cases} P^{ARINN/S}_{Netload\_up}(t+24) = P^{ARINN}_{Netload}(t+24) - \sigma_{NL}\, Q_{(1-NC)/2} \\ P^{ARINN/S}_{Netload\_low}(t+24) = P^{ARINN}_{Netload}(t+24) - \sigma_{NL}\, Q_{(1+NC)/2} \end{cases} \quad (6)$$

where $P^{ARINN}_{Netload}$ is the ARINN forecast, $\sigma_{\mathrm{NL}}$is the predicted standard deviation of the forecast errors, $Q_{(1\pm NC)/2}$ are the quantiles of the $eCDF(e/\sigma_{\mathrm{NL}})$ of order $(1 \pm NC)/2$ and $NC = 0.95$ is the nominal confidence of the PI.

3. The third method, denoted by ARINN/O is an optimal blending of the two previous models. It can be express as:

$$\begin{cases} P^{\mathrm{ARINN}/O}_{Netload\_up}(t+24) = \min\left\{P^{\mathrm{ARINN}/E}_{Netload\_up}(t+24), P^{\mathrm{ARINN}/S}_{Netload\_up}(t+24)\right\} \\ P^{\mathrm{ARINN}/O}_{Netload\_low}(t+24) = \max\left\{P^{\mathrm{ARINN/E}}_{Netload_{low}}(t+24), P^{\mathrm{ARINN}/S}_{Netload\_low}(t+24)\right\} \end{cases} \quad (7)$$

4 Regional area of interest

In the area of interest (Figure 4) there are 1985 distributed plants with a total installed capacity at the end of 2015 of 67.2 MWp (more than a third of the total installed capacity in the entire South Tyrol). The 49% of these plants have a capacity lower than 10 kWp, 38% between 10 and 50 kWp, 12% between 50 and 500 and 1% between 500 and 1000 MW. Moreover, photovoltaic is the only variable renewable energy source providing the 6.9% of the annual electric load (73 GWh over 1054 GWh), a penetration level almost equal to the national one (7% in 2015).

Therefore, this is a very good real case to study the effect of distributed PV generation on the net load variability and reserve.

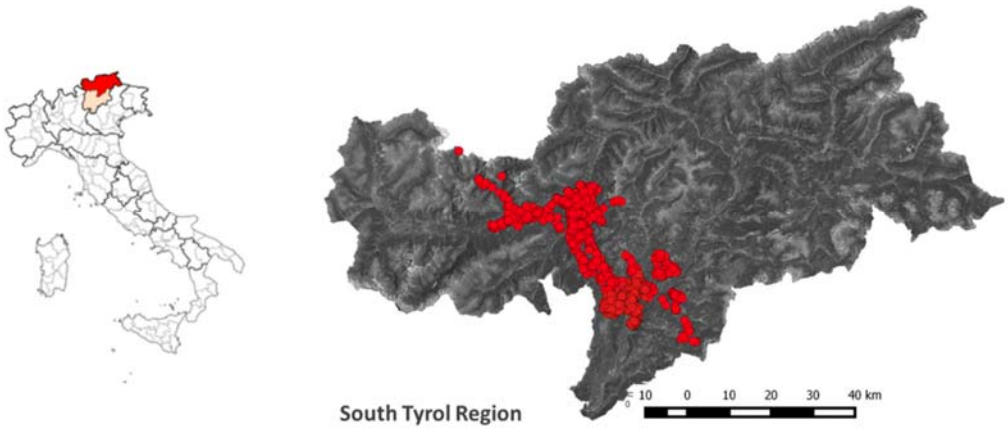

Figure 4: Geographical distribution of the PV plants (red dots) within the area of interest (around 800 km2).

5 Metrics to evaluate the accuracy and the uncertainty of the forecast

5.1 Accuracy metrics

Table1 reports the main metrics used in forecast literature to evaluate the models' accuracy.

Table 1: Accuracy metrics.

Name	Acronym and formulae
Forecast error [MW]	$e_h = \left(X^{for}(h) - X^{actual}(h)\right)$
Pearson correlation [MW]	$CORR = \frac{\mathrm{COV}(X^{for}, X^{actual})}{\sigma_{X^{for}}\, \sigma_{X^{actual}}}$
Root mean square error [MW]	$RMSE = \sqrt{\frac{\sum_{h=1}^{n} {e_h}^2}{n}}$
Mean absolute error [MW] (mean absolute imbalance)	$MAE = \frac{\sum_{h=1}^{n} \lvert e_h \rvert}{n}$
Mean bias error [MW]	$MBE = \frac{\sum_{h=1}^{n} (e_h)}{n}$

Skill score [%] (relative imbalance reduction)	$SS(ref) = 100\ (1 - \frac{MAE^{forecast\ model}}{MAE^{reference\ model}})$

where X is the considered variable, while n is the number of the yearly hours for the load or net load and is the number of yearly sun hours for PV power. The key performance indexes in MW will be also expressed in % of peak power since DSO and TSO usually adopt this unit.

It should be remarked that the MAE is exactly the yearly average of the absolute imbalance between the actual net load and the forecasted that should be accommodate by the predicted power reserve so that it can be considered the most appropriate metric to evaluate the forecast accuracy.

The skill score evaluates the accuracy improvement of the forecast model with respect to the reference model. In the case of net load forecast, it represents a measure of the absolute imbalance reduction that can be achieved using the forecast of a specific model instead of the reference prediction.

5.2 Uncertainty metrics

Table 2 reports the metrics used to evaluate the models' uncertainty.

Table 2: Uncertainty metrics.

Name	Acronym and formulae
Prediction interval coverage probability [%] (should be equal to the expected reserve valiability)	$PICP = 100\ \frac{\sum_{h=1}^{n} \delta_h}{n}$
Prediction interval average width [MW] (mean reserve)	$PIAW = \frac{\sum_{h=1}^{n} \left(X_{up}^{for}(h) - X_{low}^{for}(h)\right)}{n}$
Average width interval deviation [MW]	$AWID = \frac{\sum_{h=1}^{n}\ \delta_h^{up}\left(X^{actual}(h) - X_{up}^{for}(h)\right) +\ \delta_h^{low}\left(X_{low}^{for}(h) - X^{actual}(h)\right)}{\sum_{h=1}^{n}\left(\delta_h^{up} + \delta_h^{low}\right)}$

Max width interval deviation [MW]	$MWID = max\left\{max\{\delta_h^{up}(X^{actual}(h) - X_{up}^{for}(h))\}_h, max\{\delta_h^{low}(X_{low}^{for}(h) - X^{actual}(h))\}_h\right\}$

where X is the considered variable, while n is the number of the yearly hours for the load or net load and is the number of yearly sun hours for PV power. δ_h, δ_h^{up}, δ_h^{low} are tree Boolean functions defined as:

$$\delta_h = \begin{cases} 1 \;\; if \; X^{actual}(h) \in \{X_{low}^{for}(h), X_{up}^{for}(h)\} \\ 0 \;\; if \; X^{actual}(h) \notin \{X_{low}^{for}(h), X_{up}^{for}(h)\} \end{cases};$$

$$\delta_h^{up} = \begin{cases} 1 \;\; if \; X^{actual}(h) > X_{up}^{for}(h) \\ 0 \;\; if \; X^{actual}(h) \leq X_{up}^{for}(h) \end{cases}; \; \delta_h^{low} = \begin{cases} 1 \;\; if \; X^{actual}(h) < X_{low}^{for}(h) \\ 0 \;\; if \; X^{actual}(h) \geq X_{low}^{for}(h) \end{cases}$$

Also in this case, the key performance indexes in MW will be also expressed in % of peak power. The PICP if the observed frequency of actual data that falls inside the prediction interval. This metrics measure the reliability of the prediction interval estimation since, by definition, the PICP should be equal to the nominal confidence (PINC) that is the reserve reliability (95% in this case). The ACE represents the PICP deviation from the expected PINC, so that low ACE means high PIs reliability (since the risk provided by the model is equal to the expected ones). The PIAW represents the average uncertainty that is the average yearly reserve needed to overcome to the imbalance with the 95% of probability (5% of risk). Thus, this is the more appropriate metrics for reserve assessment.

Finally, the two new metrics AWID and MWID were introduced to measure the average and the maximum power that exceeds the expected reserve. This power should be provided by ramp reserves using high response generators able to rapidly increase or decrease their production. Also in this case, low PIAW and AWID and MWID are desirable, but low PIAW usually leads to higher deviations. Nevertheless, if enough high response capacity is available, lower PIAW are preferable since it brings to a lower prices of the dispatchable power on the balancing energy market.

6 Results

This section has been divided in three subsections. The first reports the analysis of the accuracy of the forecast models. In the second, the uncertainty of these forecasts is discussed in detail. Then, the benefit in the use probabilistic approaches in the following reserve assessment are pointed out. In the third, the dependence of the accuracy and uncertainty from the PV penetration is analyzed.

6.1 Forecast accuracy

The accuracy of the PV power forecast together with the accuracies of the respective persistence and smart persistence models are reported in Table 3. In this case, the smart persistence model achieved a lower RMSE (as expected) but a slightly higher MAE with respect to the simple persistence. The forecast model (NN) describe in section 3, reached a RMSE 7% and a MAE 4% while the reference models obtained a RMSE around 11% and a MAE of 7%. The skill score with respect to MAE of the persistence forecasts is around 40%.

Table 3: Accuracy of the day-ahead PV power forecast (in brackets the values are reported in % of the maximum power)

PV forecast accuracy										
model	**CORR**	**PEAK**	**RMSE**		**MAE**		**MBE**		**SS^{P}**	**SS^{SP}**
	[-]	[MW]	[MW]		[MW]		[MW]		[%]	[%]
P	0.82	67.2	8.15	(12%)	4.68	(7%)	0.00	(0%)		
SP	0.83	67.2	7.67	(11%)	4.93	(7%)	0.04	(0.1%)	-5.4	
NN	0.94	67.2	4.66	(7.1%)	2.82	(4%)	0.19	(0.3%)	39.8	42.8

Lorenz achieved a PV forecast RMSE of 4.1% - 4.3% for areas around 100 and 200 10^3 km^2 (Lorenz et al. (2011)) while Fonseca obtained an RMSE of 6% - 7% for areas between 30 and 70 10^3 km^2 (Fonseca et al. (2014) and (2015)). Considering that the accuracy of the regional PV forecast increases with the size of the controlled area, in [19]) was proved that the RMSE of 7.1% obtained for an area of 800 km^2 can be considered inside that “state of the art” range.

Table 4 shows the accuracy of the different models used for load and net load day-ahead forecast.

Table 4: Accuracy of the models for the day-ahead forecast, load and net load.

Load forecast accuracy										
Model	**Load peak [MW]**	**CORR**	**RMSE [MW]**		**MAE [MW]**		**MBE [MW]**		**SS^P[%]**	**SS^{SP}[%]**
P	200	0.96	8.7	(4.4%)	5.9	(3%)	-0.8	(-0.4%)	0.0	0.0
SP	200	0.97	7.4	(3.7%)	4.8	(2.4%)	0.1	(0.1%)	19.6	0.0
SARIMA	200	0.97	7.4	(3.7%)	4.4	(2.2%)	-0.6	(-0.3%)	26.4	8.4
Net load forecast accuracy										
Model	**Load peak [MW]**	**CORR**	**RMSE [MW]**		**MAE [MW]**		**MBE [MW]**		**SS^P[%]**	**SS^{SP}[%]**
P	200	0.91	11.9	(5.9%)	8	(4%)	-0.8	(-0.4%)	0.0	0.0
SP	200	0.94	9.7	(4.8%)	6.3	(3.2%)	0.2	(0.1%)	20.5	0.0
ARINN	200	0.96	8.1	(4%)	4.8	(2.4%)	-0.7	(-0.3%)	39.4	23.8

Since the load variability mainly depends on the monthly changes of the electrical demand, the day-ahead prediction can be effectively obtained also by the use of simple statistical approaches. Indeed, the simple persistence model produces MAE of 3% of the load peak. The SP, that it similar to the one actually used by the local DSO, obtains a MAE of 2.4% of the load peak, improving of almost 20% the accuracy of the P model (SS^P=19.6%). The more sophisticate time series model (SARIMA) achieves to a mean absolute error of 2.2%, improving the SP performance of only 8.4% (SS^{SP}=8.4%).

In the case of the net load forecasting, the accuracy of P model decrease of 25% with respect to the performance of the load forecast. The persistence imbalance (MAE), with the actual level of penetration, is 4% of the load peak. The SP that takes in to account the solar variability by a simple smart persistence model, achieves to an imbalance of 3.2%, obtaining a performance improvement with respect to the P model similar to the one obtained in the load forecasting (SS^P=20.5%). The ARINN model that could benefit of more accurate load and PV power predictions, achieves to an imbalance of 2.4% of the load peak. The improvement on the SP accuracy (SS^{SP}) is now 23.8%, almost three times the load forecast skill score (8.4%).

Thus, to predict the net load, an accurate forecast of the solar generation become essential, even with the 7% of penetration. The ARINN model almost completely removes the effect on the net load forecast of solar variability, obtaining a prediction accuracy (2.4%) very similar to the performance of the load forecast model (2.2%).

6.2 Forecast uncertainty

Table 5 shows the uncertainty key performance indexes achieved by the different probabilistic methods to predict PV, load and net load power.

Table 5: Uncertainty of PV, load and net load forecast models.

PV uncertainty									
Method	**PV peak [MW]**	**PICP [%]**	**PIAW [MW]**		**AWID [MW]**		**MWID [MW]**	
NN/S	67.2	95.1	16.0	(23.8%)	2.0	(3%)	15.2	(22.6%)
Load uncertainty								
Method	**Load peak [MW]**	**PICP [%]**	**PIAW [MW]**		**AWID [MW]**		**MWID [MW]**	
P/N	200	95.4	35.9	(17.9%)	6.7	(3.3%)	46.6	(23.3%)
SP/N	200	95.9	34.0	(17%)	7.8	(3.9%)	36.4	(18.2%)
SARIMA/N	200	93.9	32.6	(16.3%)	8.8	(4.4%)	44.7	(22.4%)
Net load uncertainty								
Method	**Load peak [MW]**	**PICP [%]**	**PIAW [MW]**		**AWID [MW]**		**MWID [MW]**	
P/N	200	93.7	47.3	(23.7%)	8.8	(4.4%)	40.4	(20.2%)
SP/N	200	94.1	41.5	(20.7%)	7.3	(3.7%)	39.3	(19.6%)
ARINN/E	200	95.9	35.8	(17.9%)	9.4	(4.7%)	54.9	(27.4%)
ARINN/S	200	95.7	35.0	(17.5%)	7.2	(3.6%)	44.7	(22.4%)
ARINN/O	200	94.1	28.0	(14%)	8.0	(4%)	54.9	(27.4%)

The PV forecast method (NN/S) provides a very reliable prediction interval with 95.1% of PICP (almost equal to the nominal confidence). The PIAW is 23.8% of the peak power so that the additional following reserves due to the solar generation are more than three times the PV imbalance (6.9%). As stated in section 2.2, probabilistic PV power forecast cannot be considered a complete mature technology so that it is quite difficult to compare our results with other reported in literature. Nevertheless, from Table 6, it can be noted that the developed method seems a promising approach.

Table 6: Comparison of day-ahead probabilistic error forecasting methods (PEF) available in literature in the field of irradiance and PV power predictions.

Reference	**Variable predicted**	**Approach**	**PINC [%]**	**PICP [%]**	**PIAW [% of peak power]**
(Lorenz, et al., 2009)	regional GHI	parametric PEF	**95**	**91**	-
(Ohtake, et al., 2014)	GHI	non parametric PEF	80	93	-
(Pierro, et al., 2016a)	single plant PV generation	parametric PEF	75 / **95**	86/**97**	-

(Fonseca, et al., 2015)	single plant site PV generation	parametric PEF	85/90/**95**/ 97.5	86.9/91.3/**95.3**/ 97.7	24/26/**31.5**/ 33.5
(Pierro, et al., 2017)	regional PV generation	parametric PEF with non parametric correction	75/85/**95**	76.2/87.6/**97.2**	
(Fonseca et al. 2018)	PV fleet generation	parametric and non parametric PEF	85/90/**95**/97.5	86.9/91.3/**95.5**/ 97.7	23/26.8/**32.3**/ 38.5

The reference load forecast methods (P/N and SP/N) provide a PICP of 95.4% and 95.9% (both slightly under confidence) with a PIAW of 17.9% and 17% respectively. The SARIMA/N probabilistic forecast is over confidence with a PICP of 93.9% and a PIAW of 16.3%. It is should be noted that the SP/N forecast, despite the higher PICP requires a lower ramping reserve with a MWID of 18.2% compared to the 22.4% of SARIMA/N predictions. Thus, for the assessment of the load reserves, the SP/N and the SARIMA/N methods show alternative advantages. The first is more reliable, with lower ramping reserves while the second predicts lower following reserves.

With the actual solar penetration, the reference methods (P/N and SP/N) for the net load PI assessment are both over confidence with a PICP of 93.7% and 94.1% and achieve a PIAW of 23.7% and 20.7%. The ARINN/E and ARINN/S methods are instead under confidence with 95.9% and 95.7% of PICP and achieves an average uncertainty PIAW of 19.9% and 17.5% respectively. The optimized blending method ARINN/O, even if it is slightly over confidence with 94.1% of PICP, provides a notable reduction of the uncertainty with a PIAW of 14%. For the optimized method a lower PICP was expected since the ARINN/O incorporate all the interval deviation of the two ARINN/E and ARINN/S methods. Nevertheless, the fact that with a small loss in reliability (less than 1%) the ARINN/O achieves a such lower PIAW indicates that both the ARINN/E and ARINN/S methods produce uncertainty underestimation during the same hours. It should be noted that all the ARINN methods provide a MWID higher than the SP reference method.

The outperforming methods are the ARINN/S and ARINN/O with alternative advantages. The first, is very reliable and reduces the following reserves with respect the reference methods (P and SP) of 26.1% and 15.7% providing just a small increase of the ramping reserves from 39.3% to 44.7% (MWID). The second provides a greater risk and higher ramping reserve of 54.9%. Nevertheless, the ARINN/O predicts much lower following reserves with a reserves reduction of 40.9% and 32.5% with respect the reference methods (P and SP) (almost the double of the ARINN/S method).

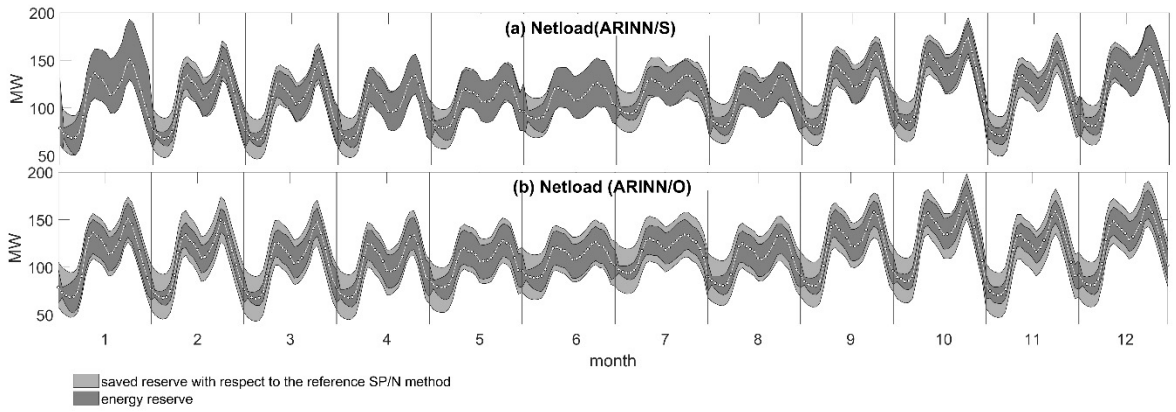

Figure 5: Monthly average of the daily following reserves and reserve reduction obtained by the use of the ARINN/S and ARINN/O probabilistic forecast instead of the SP/N prediction.

Figure 5 shows the saving in reserve that can be achieved using more accurate probabilistic methods instead of traditional statistical approach such as SP/N.

In conclusion, while in absence of solar generation the SP/N could provide an acceptable reserve estimation (see load uncertainty in *Table 5*), at the actual level of penetration more sophisticate methods become essential to limit the following reserve (see net load uncertainty in *Table 5*).

6.3 Analysis of forecast accuracy and uncertainty at different level of solar penetration

Six different levels of penetration were chosen in this study: no PV generation, 7% (actual penetration), 15% (double of the actual value), 22% (the value expected from the Italian Strategic Energy Plan for Italy at 2030), 30% (the level that it is usually assumed as a critical value for the hosting capacity) and finally the 45% (corresponding to the maximum Building Integration PV capacity in the region[2]).

Figure 6 shows the values of the key performance indexes of the forecast methods at different solar penetration.

The absolute imbalance between the actual and predicted net load change (MAE) of the models P, SP and ARINN grows from 4%, 3.2% and 2.4% of the load peak at the actual penetration to 8.8%, 7.2% and 4.6% at the 45% of penetration (Figure 6 (a)).

[2] EURAC research institute, solartirol, http://webgis.eurac.edu/solartirol/

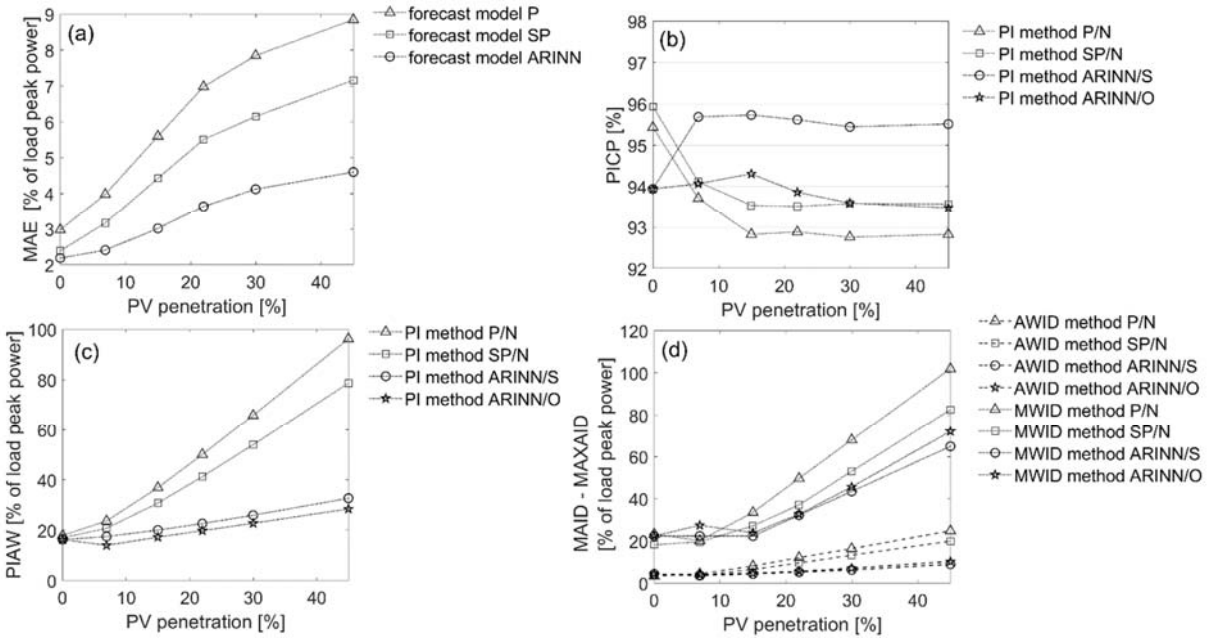

Figure 6: MAE, PICP, PIAW, AWID and MWID vs PV penetration.

At the different penetration level, almost all the methods P/N, SP/N, ARINN/S and ARINN/O are over confidence with PICP lower than the expected reliability (95%). Only the ARINN/S method shows a higher reliability when the penetration is different from zero (Figure 6 (b)). The average following reserves (PIAW) estimated by the four methods increase from 23.7%, 20.7%, 17.5% and 14.0% to 96.2%, 78.7%, 32.7%, and 28.5% when the penetration grows from the actual level to 45%. In particular, it should be noted that, at penetration greater than the actual the difference between the PIAW obtained by the P/N and SP/N methods and by the ARINN/S and ARINN/O methods increases dramatically (Figure 6 (c)). Also the average and maximum ramping reserve (AWID and MWID) obtained by the reference models are always higher than the ones achieved by the probabilistic approaches when the penetrations is greater than 7% (Figure 6 (d)).

7 Forecasting conclusion and outlook

The Eurac institute studied the impact of the distributed solar generation on the observability of the power distribution grid from the point of view of the accuracy and uncertainty of the day ahead prediction. In this contest, higher grid observability means lower imbalance between the electric demand and the power supply (net load prediction) and lower following reserves that should be held for the next day to accommodate this imbalance and stabilize the grid frequency and voltage.

The study was performed on an area of the South Tyrol region under control of a local DSO using real load and PV generation data with an hour granularity (year 2015). In the considered area the PV generation provided the 7% of the yearly electric demand and solar is the only variable energy source. Therefore, this is a good case study for the purpose of the work.

It was proved:

In absence of PV generation, the electric demand can be predicted with an acceptable accuracy and uncertainty also with simple statistical method based on historical data. Thus, this method generates reasonable values of imbalance and reserves. In particular, the statistical method and a more sophisticate probabilistic approach (that make us of more accurate PV forecast) shows

alternative advantage. The first obtains a more reliable following reserve estimation (i.e. a risk lower than expected) and a lower need of ramping reserves. The second achieves to a lower imbalance and following reserves.

Also with only the 7% of PV penetration, imbalance and reserves predicted by statistical forecast method grows considerably because of the solar generation. To contain imbalance and reserves the use of the probabilistic approach provided sensible advantages. It reduces the imbalance of 24% and the following reserves of 32%. Nevertheless, also in this case, the probabilistic model is slightly less reliable and forces the use of higher ramping reserves with respect to statistical approach.

At higher level of PV penetration, the use of more accurate PV and net load models becomes essential to limit imbalance and reserves. Indeed, with the grows of the solar penetration, imbalance and reserves obtained by statistical approach increases dramatically. In this case, the probabilistic approach will be always the best methods both in terms of imbalance, following reserves reliability, following and ramping reserves amount.

Future works will be to extend this study to the whole Italy using the data provided by the Italian TSO (Terna). Thus, the impact of solar generation over the Italian imbalance will be evaluated for different PV penetration levels and the energetic and economic benefit in using accurate forecast methods will be quantified.

8 Power Systems observability and synchronized measurements

In this paragraph, we introduce a more formal definition of observability in power systems context connected to the state estimation (SE) practice. We briefly introduce what state estimation and how the synchronized measurements can help to improve observability and accuracy for SE.

8.1 State Estimation and observability

In order to identify the current operating state of the system, state estimators facilitate accurate and efficient monitoring of operational constraints on quantities such as transmission or distribution line loadings or bus voltage magnitudes. These quantities provide a reliable real-time data base of the system for security assessment functions to analyse contingencies and to determine any required corrective actions [27].

The state estimators include different functions such as [27]:

- Topology processor
- Observability analysis
- State estimation solution
- Bad data processing
- Parameter and structural error processing

The observability analysis is the pre-requirement for the unique state estimation solution. In particular, it determines if the available measurements in the system are enough to obtain the state estimation solution. Moreover, this type of analysis identifies the unobservable branches and the observable island in the system if any exists.

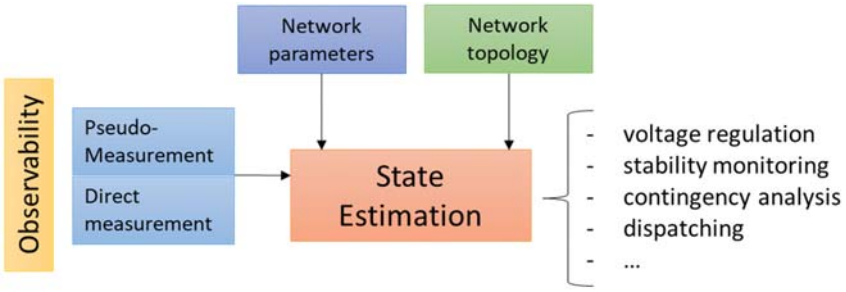

Figure 7 – State estimation inputs and possible applications

To better explain this concept let us consider a network composed by N buses and B lines. Generally, the state of the network is modelled by $x = [\theta^T, V^T]^T$ where θ^T is the vector of the voltage phasor angles at all buses and V^T is the vector of the N bus voltage magnitude. In general, the state of the network can be observed through the well-known measurements model [27] reported below:

$$\tilde{y} = h(x) + \varepsilon_y = \begin{bmatrix} P_{flow} \\ Q_{flow} \\ P_{inj} \\ Q_{inj} \\ V \\ \theta \\ I \\ \beta \end{bmatrix} + \varepsilon_y \tag{8}$$

Where h(x) is a nonlinear function of the state variables; P_{flow} and Q_{flow} are the real and reactive power flowing through the network; P_{inj} and Q_{inj} ate the vectors of real and reactive power injected at each bus; V and θ are identity functions of the state and I and β are the magnitude and phases of the line currents. The vector ε_y includes all the measurement uncertainty contributions. The explicit expression of these measurements related to the two-port π-model of network branch (as reported below) are available in the literature [27].

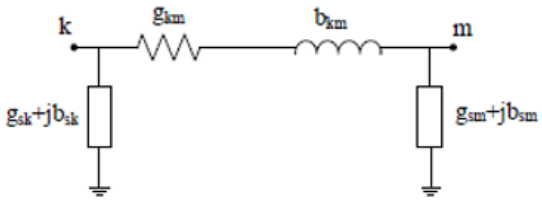

Figure 8 – Two port π-model of a network branch [27].

In practice when the set of available real-time measurements is sufficient to allow a calculation of the system state vector, the system is *observable*, otherwise is unobservable.

The typical state estimator is based on Weighted Least Squared (WLS) algorithm and well-described in [28]. When the WLS definition of the system state is given, the measurements system in (X) should have N-1 measurements available in order to be solved, otherwise the system is not observable, and the solution cannot be found. When this happen, additional meters may have to be placed in particular locations. Even if the mathematical representation and the concepts behind the state estimation and observability are essentially the same for transmission and distribution systems, the structure and the observability is very different. Indeed, transmission systems are characterized by few nodes and lines connected in a meshed topology where the number of measurements devices are typically enough to estimate the state of the grid. The classic state estimation has been conceived for the transmission system, where

the transmission system operator (TSO) based on the data collected into the SCADA are able to estimate online the voltage magnitude and angle in each node. Conversely, the distribution systems present several nodes higher than the number of available meters, they have usually a radial topology and an increasing number of distributed generations. All these aspects contribute to make the distribution grids usually unobservable and to do not find the state estimation solution. For this reason, as reported in [29] it is common at distribution level to use historical data as additional measurements to achieve the observability requirements. These data are usually called pseudo-measurements and are affected to high uncertainty contributions as reported in [29] and can be based on the monthly average values of power meters. Another possible approach should be based on the use of load or production forecasting to estimate the values of the power injected or consumed through the grid. In this case the uncertainty related to the values will depend on the used algorithm and on the time-resolution and horizon of the forecast.

It has been demonstrated in several work how the measurements accuracy can impact on the accuracy of state estimation. Since the knowledge of the grid state is used for the major operation of the grid itself as shown in these pictures inspired by [31] it is clear how better estimation correspond to a better control and usually to a minor cost of grid management.

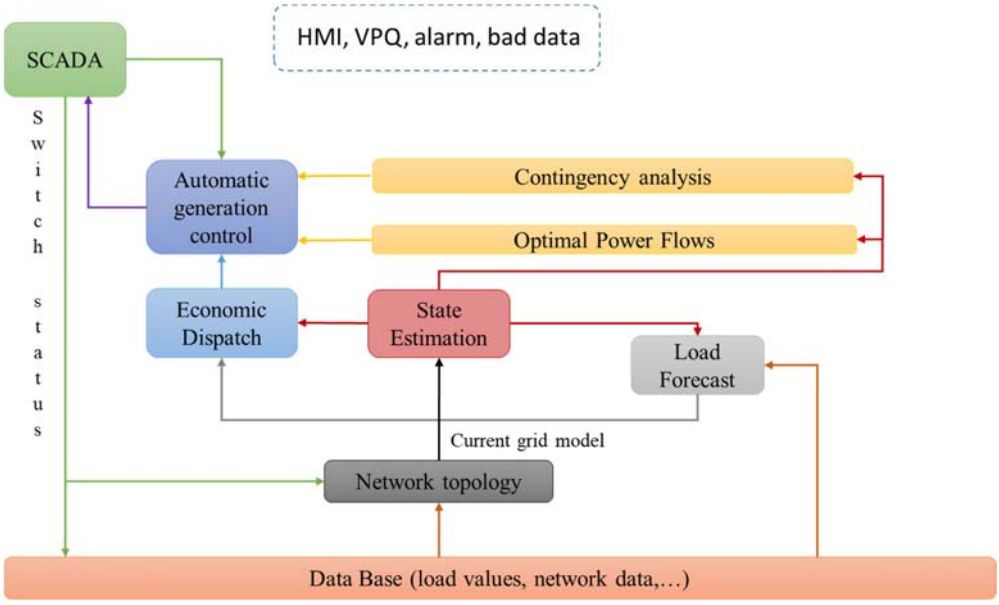

Figure 9 – Schematic representation of monitoring and control centre of electricity grid [30].

For this reason, in the last years, a new instrumentation device, able to provide worldwide synchronized measurements is playing a key role not only for state estimation but for a multitude of grid applications.

8.2 Synchronized measurements in power systems

In modern power systems the high increase of RES, the penetration of non-linear loads (such as electric vehicle) and the introduction of storage for self-consumption or energy balance require not only dynamic and advanced monitoring and controlling techniques but also frequent and accurate knowledge of the state of the grid. In the last year these functions have been supported by the so-called synchronized measurements or better synchrophasor provided by a device called phasor measurement unit (PMU).

The PMU is an instrument able to measure amplitude, phase, frequency and rate of change of frequency (ROCOF) of voltage and current waveforms synchronized with a common reference

time through a GPS receiver and referred to the Universal Coordinated Time (UTC). The first prototype of PMU has been realized at Virginia Tech around 1980s [32]. At present, PMUs by different manufacturers may differ in various important aspects. However, the architectural structure and the general functions are similar, and they are reported in [32]. For completeness, we report here the signal model and the synchrophasor definition and we remand for additional details to the wide literature.

Commonly, in AC power system a voltage or current waveform z(t) of nominal frequency f0 (i.e. 50 Hz for European countries or 60 Hz for U.S.) can be expressed as:

$$z(t) = A\cos(2\pi f_0 t + \alpha) \tag{9}$$

Where A is the amplitude and α is the initial phase. This sinusoidal waveform can be represented through its complex phasor given by

$$\hat{Z} = \frac{A}{\sqrt{2}} e^{j\alpha} \tag{10}$$

A synchronized phasor of the electrical signal in (9) is the value Z in at a known reference time tr synchronized with the Coordinated Universal Time (UTC) [33]. In the synchrophasor Standard, i.e. C37.118.1, is reported the convention for synchrophasor representation which for simplicity we report below. On the left, the synchrophasor angle is 0 degrees when the maximum of the signal occurs at the UTC second rollover, on the right the synchrophasor angle is -90 degrees when the positive zero crossing occurs at the UTC second rollover. The concept is represented below in Fig. 10.

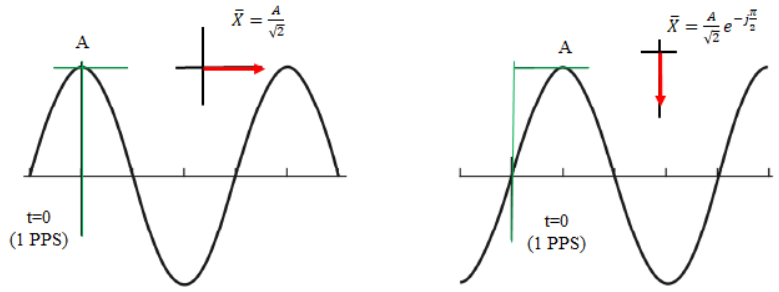

Figure 10 – Convention for synchrophasor representation [32].

8.3 Improve PV observability with PMU

As already said, the observability of distribution grid is quite difficult due to the lack of measurement point with respect to the number of grid nodes. Moreover, at distribution level there are also the major part

For instance, PMUs can greatly improve state estimation accuracy and observability even in the presence of PV plants [34]. One feature that has not been well investigated yet, is the capability of PMUs to exploit more efficiently the available solar energy by optimizing the connection and disconnection of photovoltaic (PV) plants to/from the grid. As known, the DC/AC conversion process as well as the injection of PV power into the grid pose delicate issues. At the moment, one of the main reference documents defining the guidelines to interconnect distributed generators with the grid is the IEEE Std. 1547 [35], [36]. However, since the Distribution System Operators (DSOs) are responsible for the stability of a network, the DSO policies are usually quite conservative, thus decreasing the efficiency of distributed generation resources (DERs). This problem is emphasized by the few measurement points available in the existing monitoring

infrastructures. Adding PMUs at the points of common coupling (PCCs) could be instead beneficial both to improve network observability and to enhance PV power injection management. Moreover, one of the main protection issues is related to islanding control, which requires an effective and reliable connection and disconnection of PV sources. Unlike classic synchronous generators, the PV sources exhibit high-speed response (low inertia) and large power ramps, even in the absence of transient events [37]. Nowadays the common practice of distribution system operators (DSO) in case of problems is just PV curtailment, which is a very conservative and inefficient policy. This approach is also partially due to the lack of measurement points, which makes the grid observability a challenge. Benefits for islanding control and for curtailment mitigation can result from the inclusion of PMU into PV inverters as reported in [38]. As reported in the literature, they can support several applications such as state estimation and grid observability analysis even in presence of PV generators [39]. Currently, the inclusion of synchrophasor in PV inverter is a perspective feature but could have significant advantages to both grid operator and PV owner.

References

[1] E. Ela, M. Milligan and B. Kirby, "Operating Reserves and Variable Operating Reserves and Variable Generation," NREL, 2011.

[2] H. Alfares and M. Nazeeruddin, "Electric load forecasting : literature survey and classi®cation of methods," *Internationa l Journal of Systems Science,* vol. 1, no. 33, pp. 23-34, 2002.

[3] T. Hong and S. Fan, "Probabilistic electric load forecasting: A tutorial review," *International Journal of Forecasting,* vol. 32, pp. 914-938, 2016 .

[4] A. Kaur, L. Nonnenmacher and C. Coimbra, "Impact of onsite solar generation on system load demand forecast," *Energy Conversion and Management,* vol. 75, pp. 701-709, 2013.

[5] J. Antonanzas, D. Pozo-Vázquez, L. Fernandez-Jimenez and F. J. Martinez-De-Pison, "The value of day-ahead forecasting for photovoltaics in the Spanish electricity market," *Solar Energy,* vol. 158, pp. 140-146, 2017.

[6] F. Bignucolo, A. Raciti, B. Rossi and A. Zingales, "Management of Renewable Generation Plants: Imbalance Costs and Local Storage Systems," in *AEIT Annual Conference*, 2013.

[7] M. De Giorgi, P. Congedo, M. Malvoni and D. Laforgia, "Error analysis of hybrid photovoltaic power forecasting models: A case study of mediterranean climate," *Energy Conversion and Management,* vol. 100, p. 117–130, 2015.

[8] C. Brancucci Martinez-Anido, B. Botor, A. Florita, C. Draxl, S. Lu, H. Hamann and B. Hodge, "The value of day-ahead solar power forecasting improvement," *Solar Energy ,* vol. 129, p. 192–203, 2016.

[9] H. Holttinen, M. Milligan, E. Ela, N. Menemenlis, J. Dobschinski, B. Rawn, R. Bessa, E. Gómez-Lázaro and N. Detlefsen, "Methodologies to Determine Operating Reserves Due to Increased Wind Power," *IEEE TRANSACTIONS ON SUSTAINABLE ENERGY,* vol. 3, no. 4, 2012.

[10] K. Hreinsson, M. Vrakopoulou, G. Andersson and M. Student, "Spinning and Non-spinning Reserve Allocation for Stochastic Security Constrained Unit Commitment," *18th Power Systems Computation Conference,* 2014.

[11] N. Rajbhandari, L. Weifeng, D. Pengwei, S. Sharma and B. Blevins, “Analysis of net-load forecast error and new methodology to determine Non-Spin Reserve Service requirement,” in *IEEE Power and Energy Society General Meeting (PESGM)*, 2016.

[12] J. Andrade, Y. Dong and R. Baldick, “Impact of Renewable Generation on Operational Reserves Requirements: When More Could be Less,” Energy Institute of the University of Texas, Austin, 2017.

[13] Y. Makarov, R. Guttromson, Z. Huang, K. Subbarao, P. Etingov, i. B. Chakrabart and J. MA, “Incorporating Wind Generation and Load Forecast Uncertainties into Power Grid Operations,” 2010.

[14] Hamann Hendrik, F., “A Multi-scale, Multi-Model, Machine-Learning Solar Forecasting Technology,” U.S. Department of Energy, 2017.

[15] . J. Fonseca, T. Oozeki, H. Ohtake, T. Takashima and K. Ogimoto, “Regional forecasts of photovoltaic power generation according to different data availability scenarios: a study of four methods.,” *Progress in Photovoltaics: Research and Applications,* vol. 23 (10), pp. 1203-1218, 2015 .

[16] M. Zamo, O. Mestre, P. Arbogast and O. Pannekoucke, “A benchmark of statistical regression methods for short-term forecasting of photovoltaic electricity production part I: Deterministic forecast of hourly production,” *Solar Energy,* no. 105, pp. 792-803., 2014a.

[17] B. Wolff , J. Kühnert , E. Lorenz , O. Kramer and D. Heinemann , “Comparing support vector regression for PV power forecasting to a physical modeling approach using measurement, numerical weather prediction, and cloud motion data,” *Solar Energy,* vol. 135, pp. 197-208, 2016.

[18] M. Pierro, M. De Felice, E. Maggioni, A. Perotto, F. Spada, D. Moser and C. Cornaro, "Multi-Model Ensemble for day ahead prediction of photovoltaic power generation," *Solar Energy,* vol. 134 , p. 132–146, 2016a.

[19] M. Pierro, M. De Felice, E. Maggioni, D. Moser, A. Perotto, F. Spada and C. Cornaro, “Data-driven upscaling methods for regional photovoltaic power estimation and forecast using satellite and numerical weather prediction data,” *Solar Energy,* vol. 158, pp. 1026-1038, 2017.

[20] J. G. Fonseca, T. Oozeki, H. Ohtake, T. Takashima and O. Kazuhiko, “On the use of maximum likelihood and input data similarity to obtain prediction intervals for forecasts of photovoltaic power generation,” *Journal of Electrical Engineering and Technology,* vol. 10(3), pp. 1342-1348, 2015.

[21] M. Zamo, O. Mestre, P. Arbogast and O. Pannekoucke, “A benchmark of statistical regression methods for short-term forecasting of photovoltaic electricity production. Part II: Probabilistic forecast of daily production,” *Solar Energy,* vol. 105, pp. 804-816, 2014b.

[22] M. Almeida, O. Perpiñán, L. Narvarte, O. Perpiñ Án and L. Narvarte, “PV power forecast using a nonparametric PV model,” *Solar Energy,* vol. 115, pp. 354-368, 2015.

[23] P. M. Almeida, M. d. l. P. I. Muñoz and O. Perpiñán, “Comparative study of PV power forecast using parametric and nonparametric PV models,” *Solar Energy,* vol. 155 , p. 854–866, 2017.

[24] G. Box, G. Jenkins, G. Reinsel and G. Ljung, Time Series Analysis: Forecast and Control, 5th Edition, Wiley, 2015.

[25] . J. Zhang, . B. Hodge, S. Lu , H. Hamann and B. Lehman , "Baseline and target values for regional and point PV power forecasts: Toward improved solar forecasting," *Solar Energy,* vol. 122, pp. 804-819, 2015.

[26] J. Wu, A. Botterud, A. Mills, Z. Zhou, B. Hodge and M. Heaney, "Integrating solar PV (photovoltaics) in utility system operations: Analytical framework and Arizona case study," *Energy,* vol. 85, pp. 1-9, 2015.

[27] A. Abur and A. Gomez-Exposito, Power System State Estimation: Theory and Implementation, 2004.

[28] G. Barchi, Algorithms and Performance Analysis for Synchrophasor and Grid State Estimation, PhD Thesis, University of Trento, 2015.

[29] K. A. Clements, "The impact of pseudo-measurements on state estimator accuracy," in *IEEE Power and Energy Society General Meeting*, San Diego, CA, 2011.

[30] L. Schenato, G. Barchi, D. Macii, R. Arghandeh, A. V. Meier and K. Poolla, "Bayesian Linear State Estimation using Smart Meters and PMUs Measurements in Distribution Grids," in *IEEE International Conference on Smart Grid Communications 2014*, Venice, 2014.

[31] M. &. M. J. Thomas, Power system SCADA and smart grids, 2017: CRC.

[32] G. Phadke and J. A. Thorp, Synchronized Phasor Measurements and Their Applications, Springer, 2008.

[33] "IEEE Standard for Synchrophasor Data Transfer for Power Systems," in IEEE Std C37.118.2-2011 (Revision of IEEE Std C37.118-2005) , vol., no., pp.1-53, 28 Dec. 2011," pp. 1-53, 2011.

[34] D. Macii, G. Barchi and D. Moser, "Impact of PMUs on State Estimation Accuracy in Active Distribution Grids with Large PV Penetration," in *IEEE Workshop on Environmental, Energy, and Structural Monitoring Systems*, Trento, Italy, 2015.

[35] "IEEE Standard for Interconnecting Distributed Resources with Electric Power Systems," *IEEE Std. 1547-2003,* pp. 1-28, 2003.

[36] "IEEE Standard for Interconnecting Distributed Resources with Electric Power Systems - Amendment 1," *IEEE Std. 1547a-2014 (Amendment to IEEE Std. 1547-2003),* pp. 1-16, 2014.

[37] M. Mills-Price and all., "Solar generation control with time-synchronized phasors," in *64th Annual Conference for Protective Relay Engineers*, 2011.

[38] R. Nicolosi, L. Piegari and a. A. Benigni, "A smart PV inverter controller with PMU capability," in *Clemson University Power Systems Conference (PSC)*, 2016.

[39] L. I. Dulau, M. Abrudean and D. Bica, "Impact of a photovoltaic power plant connection on the power system," in *IEEE PowerTech Conference*, Eindhoven, 2015.